


## ORIGINAL ARTICLE

# Neural Coding of Contact Events in Somatosensory Cortex

Thierry Callier<sup>1</sup>, Aneesha K. Suresh<sup>1</sup> and Sliman J. Bensmaia <sup>1,2</sup><sup>1</sup>Committee on Computational Neuroscience, University of Chicago, Chicago, IL 60637, USA and <sup>2</sup>Department of Organismal Biology and Anatomy, University of Chicago, Chicago, IL 60637, USAAddress correspondence to email: [sliman@uchicago.edu](mailto:sliman@uchicago.edu)  [orcid.org/0000-0003-4039-9135](https://orcid.org/0000-0003-4039-9135)

Thierry Callier and Aneesha K. Suresh contributed equally to this study

## Abstract

Manual interactions with objects require precise and rapid feedback about contact events. These tactile signals are integrated with motor plans throughout the neuraxis to achieve dexterous object manipulation. To better understand the role of somatosensory cortex in interactions with objects, we measured, using chronically implanted arrays of electrodes, the responses of populations of somatosensory neurons to skin indentations designed to simulate the initiation, maintenance, and termination of contact with an object. First, we find that the responses of somatosensory neurons to contact onset and offset dwarf their responses to maintenance of contact. Second, we show that these responses rapidly and reliably encode features of the simulated contact events—their timing, location, and strength—and can account for the animals' performance in an amplitude discrimination task. Third, we demonstrate that the spatiotemporal dynamics of the population response in cortex mirror those of the population response in the nerves. We conclude that the responses of populations of somatosensory neurons are well suited to encode contact transients and are consistent with a role of somatosensory cortex in signaling transitions between task subgoals.

**Key words:** neural coding, object manipulation, population coding, tactile fiber, touch

## Introduction

During manual interactions with an object, tactile signals provide precise and rapid feedback about the interface between hand and object. Several populations of mechanoreceptors in the skin convey detailed information about the timing, location, and nature of the contacts, and these signals are critical to our ability to dexterously manipulate objects (Augurelle et al. 2003; Witney et al. 2004; Johansson and Flanagan 2009). While tactile signals inform behavior at various stages of processing along the neuraxis, somatosensory cortex plays an important role in dexterous manipulation as evidenced by the fact that lesions thereof lead to severe and permanent deficits in hand use (Carlson 1981; Hikosaka et al. 1985; Xerri et al. 1998; Brochier et al. 1999; Duque et al. 2003; Schabrun et al. 2008). The precise role of somatosensory cortex in object interactions is unknown,

however. For example, whether somatosensory cortex is involved in the online control of movement is unclear, and, to the extent that it is, the time scale over which somatosensory signals inform hand movements remains to be elucidated. One role of somatosensory cortex may be to guide motor learning by conveying information about the consequences of movement (Ostry et al. 2010; Mathis et al. 2017).

To help elucidate the role of somatosensory cortex in object manipulation, we examined the responses of populations of somatosensory neurons to simulated contact events, and the dependence of these responses on the features of contact. To this end, we delivered precisely controlled indentations, designed to mimic contact with an object, to the palmar surface of the hand of Rhesus macaques while recording the activity evoked in somatosensory cortex using chronically implanted arrays of electrodes. Our goal was to understand how the onset

and offset of contact—during which the object moves into or retracts from the skin—and its maintenance—during which contact is approximately static—are encoded in the response of populations of somatosensory neurons, and how indentation depth and indentation rate modulate neuronal responses to contact. We also investigated the degree to which the spatiotemporal dynamics of the population responses in cortex reflect their inputs from the periphery by examining the simulated response of populations of tactile fibers to these same contact events.

## Materials and Methods

### Cortical Data

#### Animals

Three male Rhesus macaques (*Macaca mulatta*), 7–9 years old and weighing 9–10 kg, participated in this study. Animal care and handling conformed to the procedures approved by the University of Chicago Animal Care and Use Committee.

#### Implants

Each animal was implanted with one Utah electrode array at a time (UEA, Blackrock Microsystems, Inc., Salt Lake City, UT) in the hand representation of area 1 (Figs 1B and 2). Monkeys A and C were implanted with one array each, whereas monkey B was implanted with a second array after the first one failed. Each UEA consists of 96 electrodes, each 1.5 mm long, with tips coated with iridium oxide, spaced 400  $\mu\text{m}$  apart, and spanning 4 mm  $\times$  4 mm of the cortical surface. The hand representation in area 1 was targeted based on anatomical landmarks. Given that the arrays were contiguous to the central sulcus and area 1 spans approximately 3–5 mm of cortical surface from the sulcus (Pons et al. 1985), few if any electrodes were located in area 2. Given the length of the electrodes, their tips terminated in the infragranular layers of somatosensory cortex, as we have previously shown in postmortem histological analysis with other animals instrumented with identical arrays (Rajan et al. 2015).

#### Stimuli

Mechanical stimuli consisted of 1-s long trapezoidal indentations delivered to the palmar surface of the hand using a high-precision custom-made tactile stimulator (Fig. 1A) (similar to the one described in detail in Tabot et al. 2013). Initially, we

delivered the stimuli by measuring the position of the hand along the vertical axis using a high-precision range finder (Accurange 200–25; Acuity Lasers, Portland, OR) and having the indenting probe traverse this distance before it followed the desired indentation trajectory. Because the monkey's hand does not remain perfectly still, however, the position of the hand relative to the indenting stimulator changed over time in unpredictable ways by tens or hundreds of microns. These gradual shifts in hand position thus made it impossible to deliver indentations at a precisely controlled depth and resulted in fluctuations in the time at which the probe made contact with the skin.

To achieve well controlled skin deflections, then, we elected to preindent the stimulator tip 500  $\mu\text{m}$  into the skin throughout the duration of each experimental session, and the indentation trajectory was delivered beyond this preindentation. This experimental decision is predicated on the fact that afferent responses to the preindentation decay away within 10–20 s, as does the resulting sensation, and afferent responses to indentations of the skin beyond the preindentation are identical to those with no preindentation (Vega-Bermudez and Johnson 1999). We compared cortical responses to actual contact events (from no contact to contact, with the probe starting position 0.5–1 mm above the finger) to the cortical responses to simulated contact (with the preindentation) and found that, while the strength and timing of the latter was more variable than that of the former, the response profiles were otherwise virtually identical (see the section entitled “Preindentation vs. actual contact” in the Supplementary Methods and Supplementary Fig. S1 for a detailed comparison). Indentation depths ranged from 150 to 2000  $\mu\text{m}$ , indentation rates from 5 to 50 mm/s, and probe diameter was 2 mm. All stimuli were reliably detectable for the animals (Callier et al. 2015), and were presented in pseudorandom order.

#### Behavioral Task

Monkeys A and B performed a tactile discrimination task in a 2-alternative forced choice paradigm. In these experiments, the animals sat facing a monitor, with their hand fixed palmar surface facing up—using Velcro straps and a drop of cyanoacrylate on the nail—to allow a custom-designed tactile stimulator to indent their skin (Fig. 1A). Eye movements were tracked with an optical eye-tracking system (MR PC60, Arrington Research, Scottsdale, AZ). On each trial, 2 indentations (10 mm/s, 2-mm

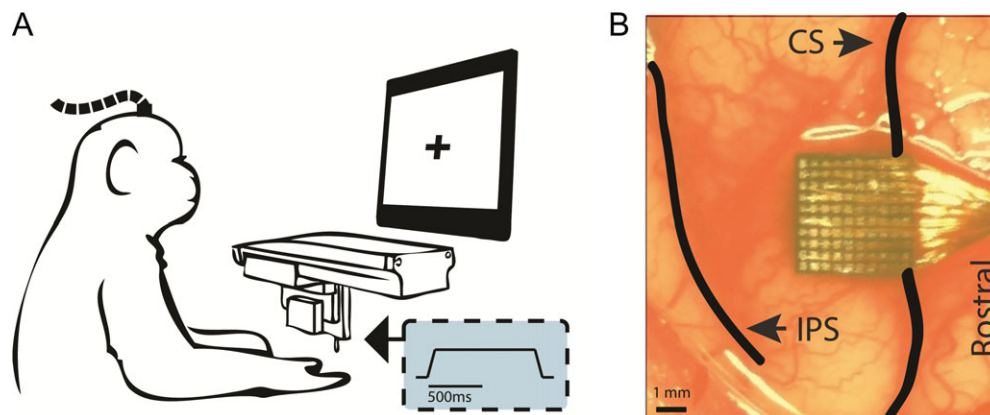


**Figure 1.** Experimental design. (A) Experimental set-up. A monkey, with head fixed and hand with palmar surface facing upwards, receives indentations to the glabrous skin. Inset: temporal profile of the mechanical indentations (depicting depth). (B) Location of monkey A's array relative to the central sulcus (CS) and intraparietal sulcus (IPS), representative of the location of all the implanted arrays.

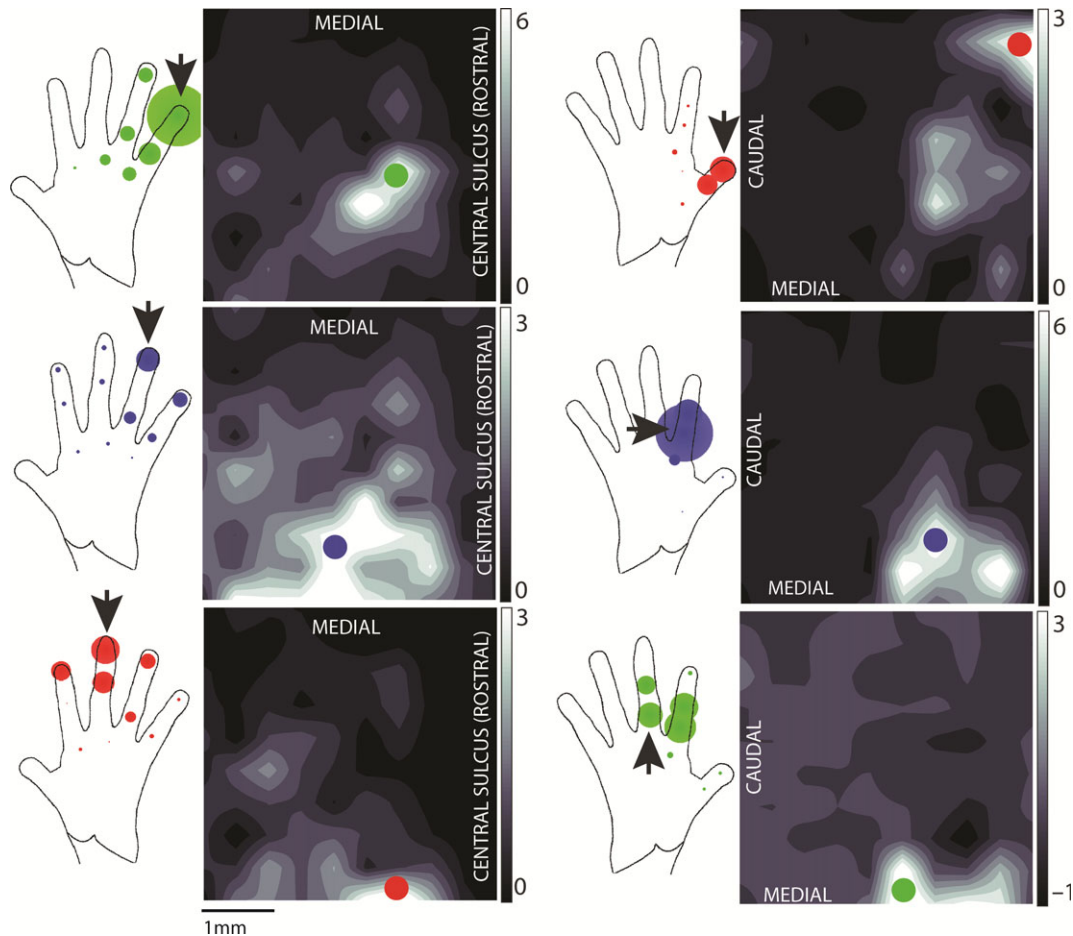


**Figure 2.** Hand representation in area 1. Distribution of neural activity on 2 different arrays (array of monkey A and the first array of monkey B in the left and right columns, respectively) evoked by stimulation at 3 skin locations (rows). The neural activity is integrated over 1200 ms following the onset of a 2-mm, 10-mm/s indentation (lasting a total of 1 s) delivered to the location indicated by an arrow on the hand diagram to the left of the heat map. The colored dot on the array represents the location of the hotzone (highest responding) electrode for that skin location. As the site of stimulation shifts in the ulnar direction (red to blue to green), the hotzone of cortical activity shifts in the medial direction, consistent with the previously established somatotopy of the hand in area 1. In the hand diagram to the left of each heat map, each colored dot represents a different site of stimulation, with the dot radius proportional to the response of the electrode marked on the array when that skin location was stimulated. The response at the electrode tends to decrease as the stimulation site moves farther from the arrow, as expected. Responses are averaged over 75+ trials in each condition.

diameter) were sequentially delivered to the skin, each 1-s long and separated by a 1-s interstimulus interval. One stimulus interval contained the standard stimulus, whose amplitude was either 150 or 2000  $\mu\text{m}$ ; and the other contained a comparison stimulus whose amplitude varied from 150 to 2000  $\mu\text{m}$  (excluding the standard amplitude). The order of presentation of the standard and comparison stimuli was randomized across trials. The monkey maintained fixation on a cross on the monitor until the end of the second stimulus presentation otherwise the trial was aborted. The animal's task was to judge which of the 2 stimuli was more intense (higher amplitude) by making a saccade to 1 of 2 visual targets placed on the left or the right of the fixation cross. Correct responses were rewarded with a drop of juice. Psychophysical performance was calculated as the proportion of trials on which the higher amplitude stimulus was correctly judged as more intense.

Additional recordings were obtained from monkeys B and C under similar circumstances, except that the animals performed a visual motion tracking task to keep them alert (see Supplementary Fig. S2 for the stimulation sites used in these experiments). The goal of these recordings was to investigate

the effects of indentation rate on cortical responses. For these measurements, the stimulator probe tip was 2 mm in diameter and indentation rates were 5, 10, 20, or 50 mm/s, thereby spanning the range of typical interactions with objects during activities of daily living (estimated from previously published interaction data (Kim et al. 2011)). To verify that responses evoked when tactile stimuli were behaviorally irrelevant were similar to those evoked with the animal engaged in a tactile discrimination task (for those stimulus conditions that were common to the 2 behavioral conditions), we compared the peristimulus time histograms obtained from the 2 conditions and the respective ratios of the transient response to the sustained response (see section entitled "Heterogeneity of cortical responses" in the [Supplementary Methods](#) for details on this metric). We found the response dynamics to be virtually identical and the ratio to be statistically indistinguishable across conditions (2 sample t-test:  $t[110] = 1.72$ ,  $P > 0.05$ ), in keeping with the expectation that attention exerts a negligible influence on neuronal responses in this area of cortex (Hyvarinen et al. 1980; Meftah et al. 2002). An experimental block consisted of a session, usually consisting of a few

hundred trials, in which a single skin location was stimulated, with or without the behavioral task.

### Electrophysiology Recording

We simultaneously recorded from all 96 electrodes of the UEAs using a Cerebus system (Blackrock Microsystems, Salt Lake City, UT), passed the continuous voltage signal from each electrode, sampled at 30 kHz, through a 100-Hz high-pass filter to reduce background noise, and recorded the timing of threshold-crossing events in each channel. Because we were interested in population responses, we analyzed multiunit (rather than single-unit) activity.

### Standardizing Neuronal Responses

Multiunit activity varies widely from electrode to electrode, both at baseline when no stimulus is applied, and in response to a stimulus, as might be expected given that different electrodes acquire signals from neuron groups that vary in size, sensitivity, and spontaneous firing rate. Counting spikes is therefore an inadequate gauge of evoked activity if one wishes to compare across electrodes. If the objective is to build an activation map across the cortical surface, it is necessary to correct for this source of variability. To this end, we standardized the evoked response according to the baseline activity (i.e., converted it to a z-score):

$$R_S(t) = \frac{R(t) - \mu_b}{\sigma_b}$$

where  $R(t)$  is the spike count in time bin  $t$  (whose width differed across analyses and ranged from 1 to 1200 ms),  $\mu_b$  is the mean spike count per bin during baseline, and  $\sigma_b$  is the standard deviation (s.d.) of the spike count per bin during baseline. Baseline spike count distributions were estimated from the response in the 500-ms time window preceding the first stimulus of each trial. Baseline levels were computed for each electrode and experimental block separately. Thus,  $R_S(t) = 3$  indicates a spike rate at time  $t$  that is 3 s.d. above the mean baseline spike rate for that electrode on that experimental block. We quantified the spatial extent of cortical activation by tracking the area of the array over which the neuronal activity exceeded a threshold (2 s.d. above baseline unless otherwise specified).

### Encoding Model

To quantify the relative contributions of indentation depth and indentation rate to the neural response, we fit a linear model relating the mean (time-varying) response at the hotzone electrode—that is, the electrode at which the strongest activity was observed when stimulating a specific skin location (Britten et al. 1992)—and the mean (time-varying) activated cortical surface area (threshold = 2 s.d. above baseline) for each of 12 indentations (0.5, 1, and 2 mm at 5, 10, 20, or 50 mm/s) to linear combinations of (time-varying) indentation depth and indentation rate at different time lags using least-sum-of-squares optimization. The shortest time lag allowed was 20 ms after stimulus onset to account for conduction latency from periphery to cortex, and the longest was 50 ms. The model was fit using responses beginning 500 ms before stimulus onset and ending 500 ms after stimulus offset, sampled at 100 Hz then averaged across 8 stimulation sites from monkeys B and C (4603 trials total) for each stimulus. Model parameters were fit to the responses to 11 stimuli using indentation depth only, indentation rate only, or both, then used to reconstruct the neural response to the 12th stimulus using the same stimulus

values (depth, rate, or both). This procedure was repeated with each stimulus left out, yielding 12 (cross-validated)  $R^2$  values for each model. From these models, we could assess the degree to which neural responses tracked indentation depth and/or indentation rate. Including acceleration into the model yielded only a modest improvement over indentation depth and/or indentation rate. Note, however, that most firing rate profiles featured bursts during acceleration events that likely reflect a sensitivity to acceleration. The lack of improvement in the model fit with the inclusion of acceleration is due to the fact that acceleration events in these stimuli are impulse functions at the beginning and end of the indentation and retraction ramps. The inclusion of acceleration has been shown to significantly improve model predictions of afferent firing rates to sinusoidal vibrations and band-pass noise, but the contribution of acceleration to firing rate is dwarfed by that of indentation rate (Okorokova et al. 2018).

### Signaling of Contact Timing

To study timing on a trial-by-trial basis, we examined how rapidly contact onset could be detected from neuronal responses. Because our neuronal sample was restricted to a small fraction of the activated population, results from this analysis constitute a floor on timing precision in cortex. First, we pooled single-trial activity from the 20 most responsive electrodes at a temporal resolution of one millisecond and smoothed these pooled responses over a causal time window (10 ms wide) (Fig. 6A). For each trial, responses were analyzed over a 1 second window centered on stimulus onset, and the first time bin in which the aggregate response exceeded a threshold of 14 s.d. above baseline was taken to be the time of detection for that contact event (Fig. 6B). Trials on which detection occurred before stimulus onset were counted as false alarms, and trials in which no contact event was detected were counted as misses. The timing results were robust to changes in threshold value over a range (from 8 to 22, but the lowest combined error rate—false alarms and misses—occurred close to 14) (Supplementary Fig. S6). For this analysis, we combined trials with amplitude 500, 1000, and 2000  $\mu\text{m}$  and analyzed them separately by indentation rate and skin location (4603 trials from 8 skin locations).

### Signaling of Contact Location

We assessed how rapidly information about contact location can be read out from the cortical response by tracing the evolution of the centroid of neural activity on the array over expanding integration time windows (Fig. 6C,D). On a trial-by-trial basis and for each integration time window beginning at stimulus onset, we computed the responses measured at each electrode, normalized these responses across electrodes to a maximum of 1, and selected all the electrodes that yielded responses above 0.65 (an arbitrary threshold, the value of which did not meaningfully affect the results as long as it was above 0.5). The position vectors of the remaining electrodes were weighted by their respective responses then averaged to obtain the centroid of neuronal activation on that trial. We used trials with amplitude 500, 1000, or 2000  $\mu\text{m}$  and analyzed them separately by indentation rate and skin location (4603 trials from 8 skin locations). We then computed the position of the mean centroid by averaging across trials at each indentation rate and skin location then computed the distance between these mean centroids and the reference centroid (calculated using an integration time window of 300 ms after response onset over all

trials). This distance was used as a measure of localization error for each integration time window. The 300-ms time window used to calculate the reference centroid is highly robust, encompassing the bulk of the neural response to stimulus onset at all indentation rates. For this analysis, we computed centroids across trials to mitigate our massive under-sampling of the response. The time course over which centroids stabilized was similar when these were computed based on single trials responses, but the errors were significantly higher. The trial-averaged centroid is still based on far fewer responses (hundreds per skin location) than are included over the relevant neuronal volume (tens of thousands).

### Neurometric Analysis

We wished to assess the degree to which neuronal responses evoked during the behavioral task could account for the animals' perceptual judgments. To this end, we performed 2 ideal observer analyses. In one, we computed the proportion of times the strong stimulus (standard or comparison) evoked the stronger response at the hotzone electrode. In the second, we computed the proportion of times the stronger stimulus (standard or comparison) elicited the more widespread response. For this analysis, we used a low threshold (0.5 s.d. above baseline) to achieve a more graded metric since estimates of recruitment are limited by the spatial resolution of the array; that being said, results were robust to changes in threshold over a range. These analyses yielded performance metrics that could be directly compared with those of the animals' behavior. We used 2 time windows to perform these analyses: 1) The response over a 300-ms period following stimulus onset, which encompassed the indentation ramp (200-ms duration at the largest indentation) and captured any residual phasic activity, and 2) the response during the sustained epoch, encompassing the 300-ms period beginning 400 ms after stimulus onset (at which time the phasic response had subsided). For both time windows, we corrected for response latency, ~20 ms (Fig. 7). In addition, we performed the ideal observer analysis using a time window that spanned only probe movement for each indentation amplitude (the width of which thus varied with amplitude) to isolate the contribution of the phasic response (Supplementary Fig. S11).

### Simulations of Whole Nerve Responses

We wished to compare the responses to contact events in somatosensory cortex and in the somatosensory nerves. To this end, we reconstructed the responses of all tactile nerve fibers—slowly adapting type 1 (SA1), rapidly adapting (RA), and Pacinian corpuscle-associated (PC)—that innervate the palmar surface of the hand to each of the stimuli presented in the cortical experiments. Specifically, we used a recently developed simulation of the nerve that can accurately reproduce afferent responses with near millisecond accuracy (Saal et al. 2017). In brief, the model first computes the skin's response to a time-varying stimulus impinging upon it, then generates the spiking response evoked in nerve fibers whose receptive fields (RFs) tile the skin at measured innervation densities. This simulation has been extensively validated using a variety of psychophysical and neurophysiological data sets (Goodman and Bensmaia 2017; Saal et al. 2017). Using this model, we simulated the nerve responses to the mechanical stimuli used in the cortical experiments, described above, and compared these simulated responses to their measured cortical counterparts. We delivered the simulated indentations at each location that was mechanically stimulated in the cortical experiments (see

Supplementary Fig. S2). For finger sites, we simulated responses over each respective finger, and for palm sites, we simulated responses over the entire palm (mean = 2498 fibers, stdev = 1369 fibers). For recruitment calculations, we only included SA1 and RA afferent responses. To validate the simulation, we compared simulated afferent responses to a skin indentation to their measured counterparts (see section entitled "Single unit recordings from the nerve" in the Supplementary Materials and Supplementary Fig. S7).

To compare simulated responses of tactile nerve fibers to the measured responses of cortical neurons, we computed the cross-correlation between their respective peristimulus time histograms (PSTHs) using an average for each stimulus across locations (distal finger, proximal finger, and palm; see Supplementary Fig. S10). Specifically, for each stimulus condition (12 pairs varying in indentation depth and indentation rate), we smoothed the responses, starting 500 ms before stimulus onset to 500 ms after stimulus offset, with a 20 ms Gaussian kernel and computed the correlation coefficient at the optimal lag.

To verify that the indentations were ethologically valid, we simulated the response to a time-varying indentation that resembles the skin deflection produced when an object is grasped, lifted up, and released (see section entitled "Simulating the response of the nerve during a manual interaction with an object" in the Supplementary Methods). We then compared the simulated responses of tactile nerve fibers to this naturalistic stimulus and to the trapezoidal indentations.

## Results

Using chronically implanted electrode arrays, we recorded the multiunit responses evoked across populations of neurons in area 1 when the palmar surface of the hand was indented with a punctate probe at different locations, to different depths, and at different indentation rates (Fig. 1).

### Spatial Layout of the Cortical Response

Indentation at different locations on the skin evoked activity that was localized to different regions of somatosensory cortex, usually with some overlap for adjacent skin locations (Penfield et al. 1937; Iwamura et al. 1983; Kaas 1983; Reed et al. 2008) (Fig. 2). While the magnitude of the neural response varied greatly over the course of a stimulation event and with stimulation parameters, the locus of activity remained unchanged, generally centered on a single electrode, to which we will refer as the hotzone electrode (the converse of the hotspot, or point of maximum sensitivity, of an RF). The location of the hotzone electrode followed the well-known somatotopic organization of somatosensory cortex, progressing medially and posterior along the central sulcus from the first to fifth digit. Typically, a given array would impinge upon the representation of 2–4 digits.

### Temporal Profile of the Cortical Response

First, we examined the time course of neuronal activation recorded from the hotzone electrode. Here, we focused on a single mechanical stimulus, namely a probe with a diameter of 2 mm indented 2 mm into the skin at 10 mm/s, held for 600 ms, and then retracted at 10 mm/s. In all cases, activity rose sharply, with a latency of about 20 ms after stimulus onset and remained high as long as the probe continued to move into the skin. As soon as the probe stopped moving, however, neuronal activity

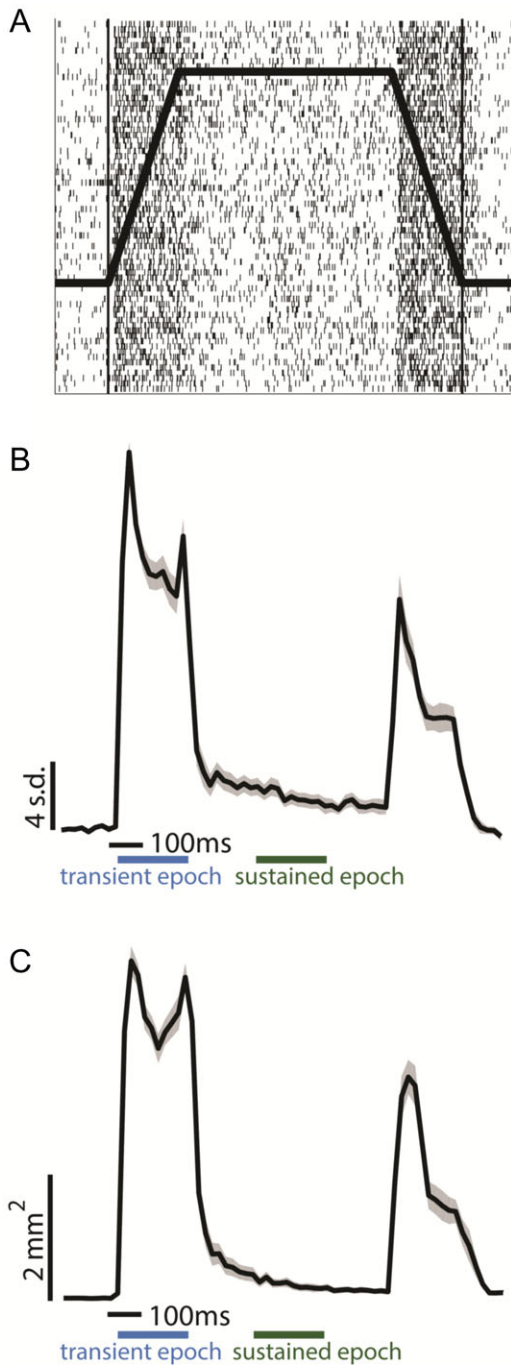


**Figure 3.** Spatiotemporal dynamics of the response. (A) Multiunit raster of the response at the hotzone electrode to 70 repeated presentations of a 2-mm, 10-mm/s indentation delivered to the little finger (Fig. 1A, top left), the profile of which is superimposed on the raster. (B) Peristimulus time histogram of the response (standard deviations above baseline mean) at the hotzone electrode to the same stimulus, averaged over 3408 trials from 28 palmar skin locations across the 4 arrays from the 3 animals (see Fig. 2 and Supplementary Fig. S2 for all contact locations). Responses were normalized to a maximum of 1 within electrodes, averaged across electrodes, then multiplied by the mean peak response across electrodes. Shaded area denotes the standard error of the mean (SEM,  $N = 28$  skin locations, time bin = 20 ms). Blue and green bars indicate transient and sustained epochs, respectively. The leftmost edge of the time scale bar indicates stimulus onset. The response to contact transients is far more prominent than that to static contact. (C) Dynamics of the spatial extent of cortical activation (surface with response greater than 2 std above baseline) as a function of time (3408 trials from 28 palmar skin locations across

abruptly dropped, often nearly to baseline despite the sustainment of the indentation (Fig. 3A,B). Probe retraction also evoked a strong response, albeit weaker than during indentation.

To quantify the magnitude of the difference between the initial burst of activity (transient response evoked during probe movement), and subsequent tonic activity (sustained response while probe is statically indented into the skin), we computed the ratio between the spike rate over the first 200 ms of the response to that over a 200-ms window beginning 200 ms after the probe had stopped moving. We found that the response at the hotzone electrode during the onset transient was on average more than 15 times stronger than its counterpart during the static period and that this ratio varied widely across electrodes/skin locations (range: 2.2 to 42.4, median: 12.0 over 28 skin locations from 4 arrays) (Fig. 3B, Supplementary Fig. S3, Supplementary Table S1; see section entitled “Heterogeneity of cortical responses” in the Supplementary Materials). Similarly, the response at the hotzone electrode during the offset transient was on average more than 8 times stronger than the sustained response (range: 0.76 to 35.0, median 6.0; Supplementary Table S1, Supplementary Fig. S3). Ratios spanned a wide range and, while they overlapped largely across skin locations, electrodes with RFs on the palm tended to exhibit relatively weaker sustained responses (Supplementary Fig. S4, Supplementary Table S1). The variation in the ratio of transient to sustained response likely reflects variation in the relative strength of the input from different classes of nerve fibers across the cortical sheet (Sur et al. 1981). For instance, the relatively weaker sustained responses in palm cortex likely reflects the lower density of slowly adapting fibers on the palm relative to their rapidly adapting counterparts (Johansson and Vallbo 1979). Heterogeneity in these and other response metrics derived from cortical responses is documented in greater detail in Supplementary Tables S1–S5.

### Spatiotemporal Dynamics of the Cortical Response

As mentioned above, activation was not limited to a single electrode but rather was distributed over an area of cortex that spanned multiple electrodes. In light of this, we examined how the spatial pattern of activation evolved over time. We found that large swaths of cortex were activated as the probe moved into the skin (Fig. 3C, Supplementary Fig. S3B). For example, a 10-mm/s indentation activated on average around 5 mm<sup>2</sup> of somatosensory cortex. During the sustained portion of the indentation, however, the area of activation was limited to a small area (a fraction of a square millimeter) centered on the hotzone electrode. As was the case with response strength, recruitment also exhibited heterogeneity in its dynamics (Supplementary Table S5). Indeed, the extent of activation at stimulus onset and offset varied over the cortical sheet, though recruitment during the transients always dwarfed its counterpart during the sustained epoch. Recruitment was more restricted for palm stimulation than for digit stimulation (Supplementary Table S5), but the comparison is limited by the small number of stimulation sites.

4 arrays). Activation area was normalized to a maximum of 1 within skin locations, averaged across locations, then multiplied by the average peak activation area across skin locations. Leftmost edge of the time scale bar indicates stimulus onset, shaded area is SEM ( $N = 28$  skin locations, time bin = 20 ms). The extent of activation is far greater during contact transients than during static contact.

## Dependence of the Cortical Response on Contact Parameters

Next, we examined the degree to which the spatiotemporal dynamics of the response depend on the features of the simulated contact event.

First, we investigated the dependence of transient responses on indentation rate. Restricting our analysis to the period of time when the probe is moving, we found that both the firing rate at the hotzone electrode and the spatial extent of the activation increased monotonically with indentation rate (Fig. 4A–F) but the

spatial distribution did not change shape—responses scaled by roughly the same amount over the extent of the array (Fig. 4G). Here, we restricted the time window over which responses were integrated to 40 ms, the duration of the transient at the highest indentation rate (2 mm traveled at 50 mm/s), so that the initial burst of activity would not be weighted more heavily for the higher velocities. This meant, however, that the total indentation depth varied with indentation rate. The results were not meaningfully changed when responses were integrated over the full transient at each indentation rate, so that total indentation depth

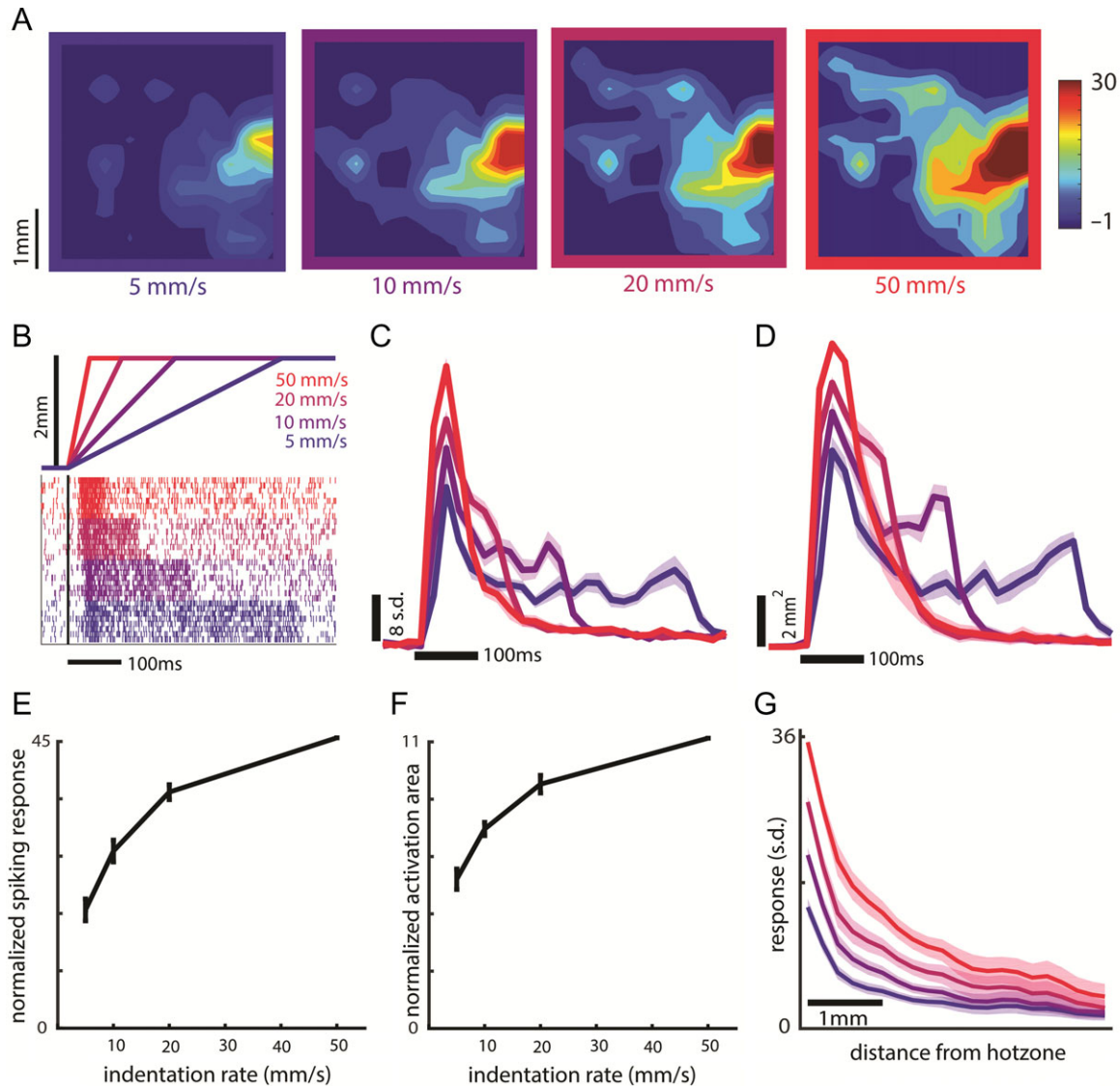


**Figure 4.** Effect of indentation rate on the transient response. (A) Heat map of neural activity during the first 40 ms of the response (starting 20 ms after stimulus onset to account for response latency) to a 2-mm indentation delivered to the second palmar pad of monkey C at indentation rates of 5, 10, 20, and 50 mm/s (40 ms is the probe movement time at the highest indentation rate; data averaged across 54 trials per indentation rate). (B) Indentation traces (top), along with the (color-matched) cortical responses (bottom). Indentation depth is constant so ramp durations increase as indentation rate decreases, as do the corresponding transient responses. (C) Time course of the response at the hotzone electrode to a 2-mm indentation at each indentation rate, averaged over 1535 trials across 8 skin locations from 2 arrays (second array of Monkey B and monkey C, same data for C–G). In panels C–G, responses were normalized as in Figure 3 ( $N = 8$  skin locations). Leftmost edge of the time scale bar indicates stimulus onset. (D) Dynamics of the spatial extent of activation evoked by a 2-mm indentation at each indentation rate. Peak activated area was normalized as in Figure 3. Leftmost edge of the scale bar indicates stimulus onset. Shaded area shows the SEM ( $N = 8$ ). Responses in C and D were calculated in 20-ms bins. (E) Mean and SEM of the cortical response at the hotzone electrode versus indentation rate during the transient for a 2-mm indentation. We used the same integration time window for each indentation rate (first 40 ms of the response starting 20 ms after stimulus onset). (F) Mean and SEM of the activated area versus probe indentation rate during the transient for a 2-mm indentation. We used the same integration time window at each indentation rate. (G) Response as a function of distance from the hotzone at the different indentation rates.

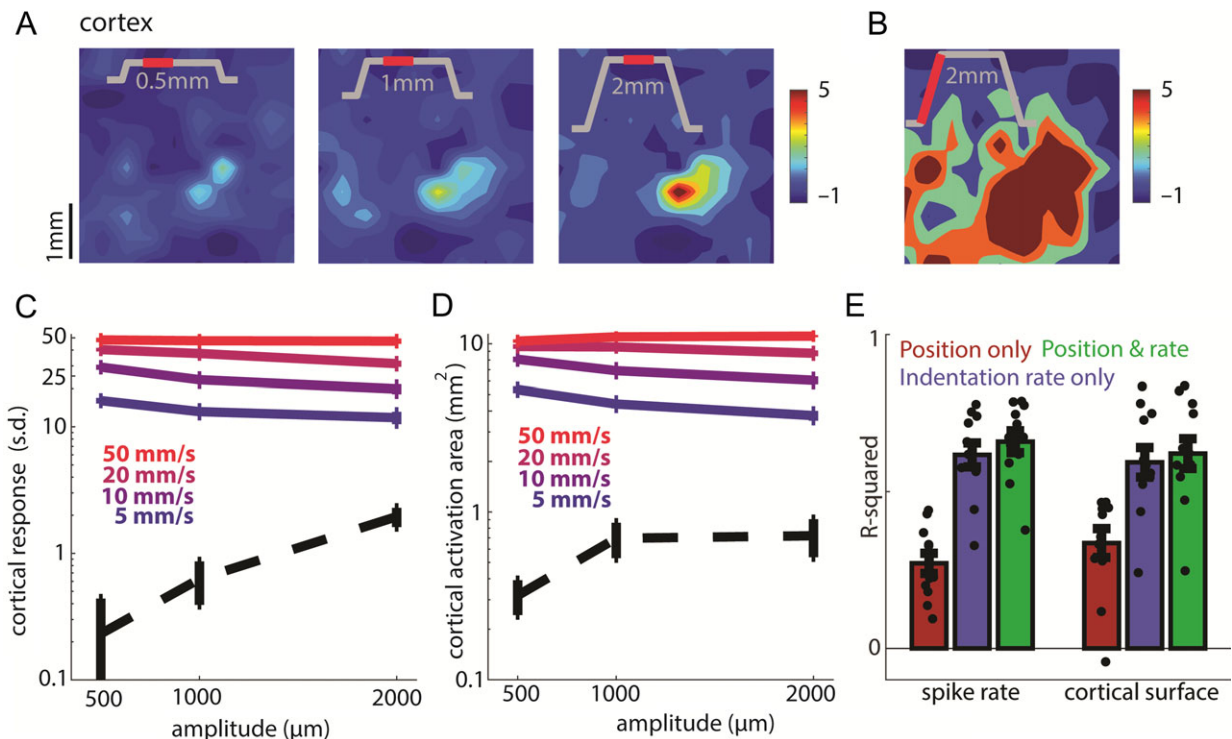


**Figure 5.** Effect of indentation depth on the sustained and transient responses. (A) Top: Spatial layout of the sustained response to 0.5-, 1-, and 2-mm indentations delivered to the little fingertip of monkey A at 10 mm/s (min 40 trials per amplitude). The inset shows the stimulus trace, the red section the relevant stimulus epoch (200 ms beginning 200 ms after the probe stopped moving, the only exception being the 2-mm, 5 mm/s indentation, for which the sustained epoch represents only the last 150 ms before probe retraction begins). (B) For comparison, spatial layout of the cortical response during contact onset of the same stimulation (the first 200 ms of the response). (C) Standardized firing rate at the hotzone electrode versus indentation depth during the transient phase (solid lines) and the sustained phase (dashed line) of the stimulus (4603 trials averaged across 8 skin locations from monkey B's second array and monkey C, same for C–E). The solid lines correspond to indentation velocities of 5, 10, 20, and 50 mm/s, and the dashed line to the sustained response averaged across trials at all velocities. Error bars show the SEM ( $N = 8$ ). Responses were integrated over the full duration of the stimulus ramp. Note the logarithmically scaled ordinate. (D) Activation area versus indentation depth for the same stimuli and epochs as in C. (E) Fit of linear models relating spike rate at the hotzone electrode (left 3 bars) and activated cortical surface (right 3 bars) to time-varying indentation depth and rate. Neuronal responses primarily track indentation rate. Dots show the individual stimuli, and error bars show the SEM ( $n = 12$  stimuli). Each color denotes different inputs used for both model training and reconstruction of the response.

was constant but ramp duration decreased as speed increased (see colored traces in Fig. 5C,D). To confirm that our firing response measures did not simply reflect increased recruitment around the electrode, we analyzed single-unit cortical data, and found that individual units increased their firing with increases in indentation rate (see section entitled “Single-electrode recordings from cortex” in the Supplementary Materials, Supplementary Fig. S5).

Next, we examined the dependence of the response on indentation depth (Fig. 5). Restricting our analysis to the sustained response period, after the transient response had subsided, we found that both the firing rate at the hotzone electrode and the spatial extent of activation increased monotonically as the amplitude increased from 500 to 2000  $\mu\text{m}$  (Fig. 5A, dashed line in Fig. 5C,D). During the transients, the modulation of firing rate and recruitment by indentation depth was weak compared with the modulation of firing rate and recruitment by indentation rate (colored traces in Fig. 5C,D). If anything, firing rate seems to decrease as amplitude increases because, as the ramp gets longer, the strong initial burst (possibly driven by an acceleration event) gets washed out and this effect counteracts the weak amplitude-dependent increase in firing rate.

To quantify the relative contributions of indentation depth and indentation rate to the neural response, we fit linear models relating time-varying firing rate at the hotzone electrode

and the time-varying spatial extent of activation (threshold = 2 s.d.) to time-varying indentation depth and indentation rate over a causal time window. For both hotzone firing rate and activated cortical area, models that included indentation depth and indentation rate yielded the best reconstruction of the neuronal response (firing rate:  $R^2 = 0.66 \pm 0.12$ ; activated area:  $R^2 = 0.62 \pm 0.17$ ). The reconstruction based on indentation rate only performed nearly as well ( $0.62 \pm 0.13$ ;  $0.59 \pm 0.16$ ), while the reconstruction based on depth alone performed far worse ( $0.27 \pm 0.11$ ;  $0.33 \pm 0.16$ ), highlighting that neuronal responses primarily track indentation rate rather than indentation depth (Fig. 5E). Models yielded marginally better performance if acceleration was taken into consideration (firing rate:  $R^2 = 0.67 \pm 0.15$ ; activated area:  $R^2 = 0.64 \pm 0.18$ ). Note, however, that acceleration has been shown to drive afferent responses, though to a far lesser extent than does indentation rate (Dong et al. 2013; Saal et al. 2017; Okorokova et al. 2018), but ramp-and-hold stimuli are ill suited to reveal the contribution of acceleration (see Materials and Methods).

### Rapid and Precise Signaling of Contact Timing

The rapid rise of the cortical response upon object contact (Fig. 6A) yields a representation that is well suited to provide precise information about the timing of contact. With this in mind, we wished to estimate how rapidly contact with an



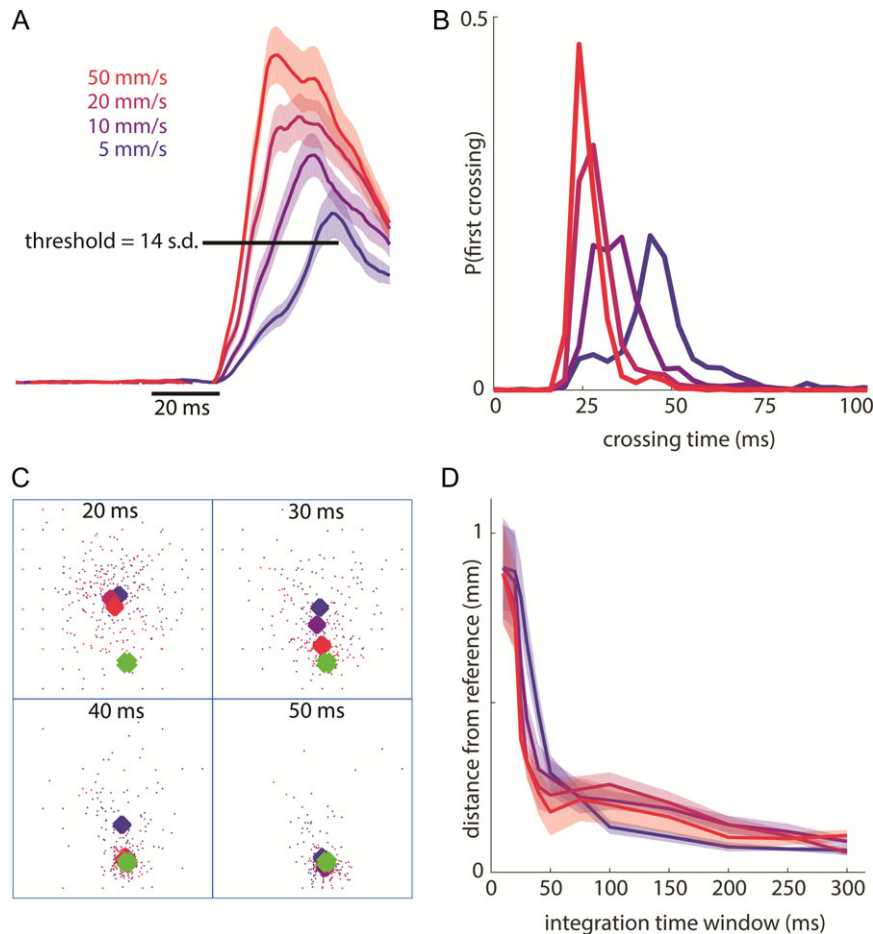


**Figure 6.** Rapid detection and localization of contact events. (A) Pooled response of the 20 most responsive electrodes (for each skin location) around stimulus onset (smoothed over a 10-ms causal window). Shaded area shows the SEM (4603 total trials across 8 stimulation sites from monkey B's second array and monkey C). Leftmost edge of the time bar indicates stimulus onset. The threshold bar indicates the minimum single-trial response to signal a contact event (used to obtain the distribution in panel B). (B) Distribution of threshold-crossing times for each indentation rate for the same trials as in panel A (grouped in 4-ms bins). (C) For one example skin location (first palmar pad of monkey C), scatter plot of centroids for single-trial responses (small dots, color-coded by indentation rate) and mean responses (large diamonds) at integration windows of 20, 30, 40, and 50 ms following stimulus onset. The square denotes the 4 mm  $\times$  4 mm array and the green diamonds shows the reference centroid (calculated using an integration time window of 300 ms across all trials). The average centroids migrate to the reference centroid location within 40–50 ms. (D) Mean distance (across same stimulation sites as in A) between the reference centroid and the average centroids (for each indentation rate) as a function of integration time. Shaded area shows SEM.

object can be detected. To this end, we assessed when the aggregate cortical activity passes a (rather stringent) threshold on a trial by trial basis. We found that we could reliably detect the stimulus less than 30 ms after onset for the most rapid indentation (Fig. 6B). Given that the time for neuronal signals to propagate from the skin of the hand to the brain is around 20 ms (Sripati et al. 2006), this signal is nearly as rapid as it could be. Importantly, even with this minuscule subset of the true cortical response, detection time was tightly distributed around its mean (e.g., at 50 mm/s, 80% of the detection times were within 6 ms of their modal value), which highlights the reliability of this contact signal. Changing the detection criterion within a wide range did not greatly affect the modal detection time, but a lower threshold led to more spurious detections while a higher threshold led to more failures to detect (Supplementary Fig. S6). A neuronal response that tracked indentation depth rather than indentation rate, and thus evolved more slowly, would yield a slower and less precise contact timing signal.

### Rapid and Precise Signaling of Contact Location

The location of contact is known to be encoded in the location of the evoked activity in somatosensory cortex. The most convincing evidence for this neural code is that microstimulation of neurons with RFs at a specific location on the body evokes sensations referred to that location (Tabot et al. 2013; Flesher et al. 2016). However, the spatial extent of activation is dependent on stimulus parameters, especially indentation rate, while the perceived location of contact remains consistent (as long as the stimulus is sufficiently above threshold (Johnson and Phillips 1981; Gibson and Craig 2006)). We wished to assess the degree to which the centroid of neuronal activation evoked at a specific contact location was consistent across indentation rates and to characterize the time course over which it stabilized. We found that, at the highest indentation rate, the centroid of activation became stable within about 40 ms after contact (Fig. 6C,D). In other words, the contact location was signaled almost as rapidly as it could be given the minimal

response latency of around 20 ms. Given how dramatically the neuronal response was under-sampled, this constitutes an upper bound on timing and a lower bound on precision.

### Relating Neuronal Responses to Behavior

Next, we assessed whether the responses of somatosensory neurons could account for the animals' amplitude discrimination performance. We used an ideal observer analysis to compute the discriminability based on neuronal responses measured as the animals performed the task. Specifically, we computed the proportion of times the comparison stimulus produced the stronger response and compared the resulting neurometric functions to the proportion of times the animal judged the comparison stimulus to be more intense. For the neurometric analysis, we used an epoch encompassing the transient response or one that included only the sustained response. We found that neurometric performance was best when we used a response epoch that included the transient phase and that it was comparable to the performance of the animal on the amplitude discrimination task (Fig. 7A,B, compare red trace to blue trace). In contrast, neurometric performance was poor when only the sustained period was used

(Fig. 7A,B, green trace). In other words, more information about the stimulus is conveyed in the transient response than in the sustained one. Note that, because the indentation rate was the same at all amplitudes, increases in amplitude were associated with increases in the duration of the ramp. In principle, then, the animals could have performed this task by estimating the duration of the ramp. However, human subjects have been shown to have a poor sense of the temporal profile of an indentation and feel as though the indentation continues even after the probe has stopped moving (Poulos et al. 1984). Furthermore, after having performed a mechanical discrimination task, Monkeys A and B switched to a task in which they judged the relative amplitude of intracortical microstimulation (ICMS) trains—which did not have onset or offset ramps—and generalized to this new modality instantly (Tabot et al. 2013). In light of these observations, it is unlikely the animals used ramp duration to make their discrimination judgments. Neurometric performance based on responses restricted to probe movement far exceeded the behavioral performance as might be expected given that the duration of the response epoch increases with amplitude (Supplementary Fig. S11).

We find, then, that the best discrimination performance is supported by integrating indentation rate—encoded in the

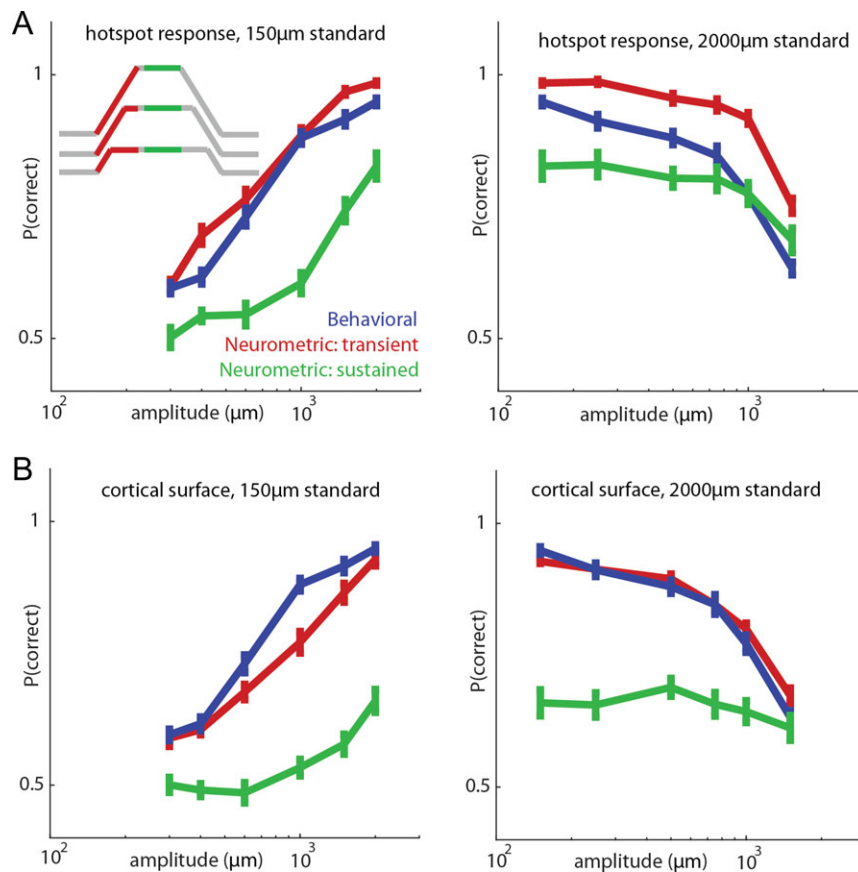


**Figure 7.** Relating neuronal responses to behavioral performance. (A) Performance of the animals (blue) and that of an ideal observer based on the onset transient response (red, 300 ms window for all stimuli) and the sustained response (green, 300 ms window for all stimuli) at the hotzone electrode for a 150- $\mu\text{m}$  standard stimulus (left, 5645 trials from 17 skin locations from monkey A and monkey B's first array) and 2000- $\mu\text{m}$  standard stimulus (right, 6546 trials from 17 skin locations over the same 2 arrays). Inset shows the stimulus trace with color-coded stimulus epochs for 3 example stimuli (not drawn to scale). All stimuli in the behavioral task were delivered at 10 mm/s. Error bars denote the standard error of the mean ( $n = 17$  skin locations). Behavioral performance approximately matches the neurometric performance based on the onset responses but is underestimated from the sustained response. If only the transient response is used, performance is even better (supplementary Fig. S11). (B) Analogous ideal observer analysis based on activated cortical surface (number of channels with neuronal response above 0.5 s.d.).

phasic response—rather than by directly encoding indentation depth—reflected in the tonic response. Indeed, the phasic burst during the on-ramp is longer—and thus comprises more spikes—at long ramp durations, and the strength of that burst can account for the animal’s performance. We performed the same analysis using area of activation rather than firing rate and obtained analogous results (Fig. 7B), though firing rate yielded better performance than did activation area.

Note that, from these behavioral data, we cannot conclusively establish the neural code that underlies task performance. Indeed, the animals’ judgments could rely on a combination of population spike rate and recruitment, for example, and the choice of integration time window—300 ms—was quasi arbitrary (chosen to span the duration of the longest ramp and any residual phasic activity). The important conclusions is that the transient response information conveys far more information about stimulus intensity than does the sustained one.

### Spatiotemporal Dynamics of the Response in the Peripheral Nerve

Finally, we wished to assess the degree to which cortical responses reflect their peripheral inputs. To this end, we simulated the response to all afferents activated by an indentation with identical parameters as the ones described above for the cortical experiment. We found that hundreds of afferents were activated, and that their aggregate response during the transients dwarfed that during the sustained portion of the stimulus, which was, again, remarkably weak (Fig. 8A, also shown for measured responses in Supplementary Fig. S7A). The dominance of the transient response is due to the fact that RA and PC fibers only respond to changes in skin indentation, leaving only SA1 fibers to respond to the sustained indentation, and even these fibers respond more strongly

to skin deflections (Knibestöl 1973, 1975). We also computed the transient-to-sustained-response ratio for aggregate peripheral responses to a probe with a diameter of 2 mm indented 2 mm into the skin at 10 mm/s, and found that transient responses were on average nearly 12 times (range 5.12–45.37, median 9.2, see Supplementary Table S6) stronger at stimulus onset and more than 5 times stronger at stimulus offset than sustained responses, similar to their cortical counterparts (means of around 15 and 8 for onset and offset, respectively, see above). As was found in the cortical responses, these ratios tended to be larger for the palm than for the distal digits, reflecting differences in the relative proportions of slowly adapting and rapidly adapting nerve fibers terminating in the different hand regions.

We then examined how the spatial pattern of activation evoked in nerve fibers by a skin indentation evolved over time. To this end, we computed the area of a polygon that contains all (simulated) SA1 and RA afferents activated by the stimulus as a function of time. We excluded PC fibers in this computation because their RFs are so large as to span most of the hand, and a given PC fiber is activated by touch almost anywhere on the hand. As was found in cortex, afferent activation during stimulus transients was distributed across wide swaths of skin around the probe, while activation during the static phase was localized to a small patch of skin under the probe (Fig. 8B,C).

Next, we examined the dependence of the nerve response on the features of the contact event. We found that the strength and spatial extent of simulated afferent responses during the transient phase of the stimulus were only weakly modulated by indentation depth, whereas the afferent responses during the transient phase were strongly modulated by indentation rate (Supplementary Figs S8 and S9), as was found in cortex.

To quantify the similarity between peripheral and cortical responses, we computed the cross-correlation between

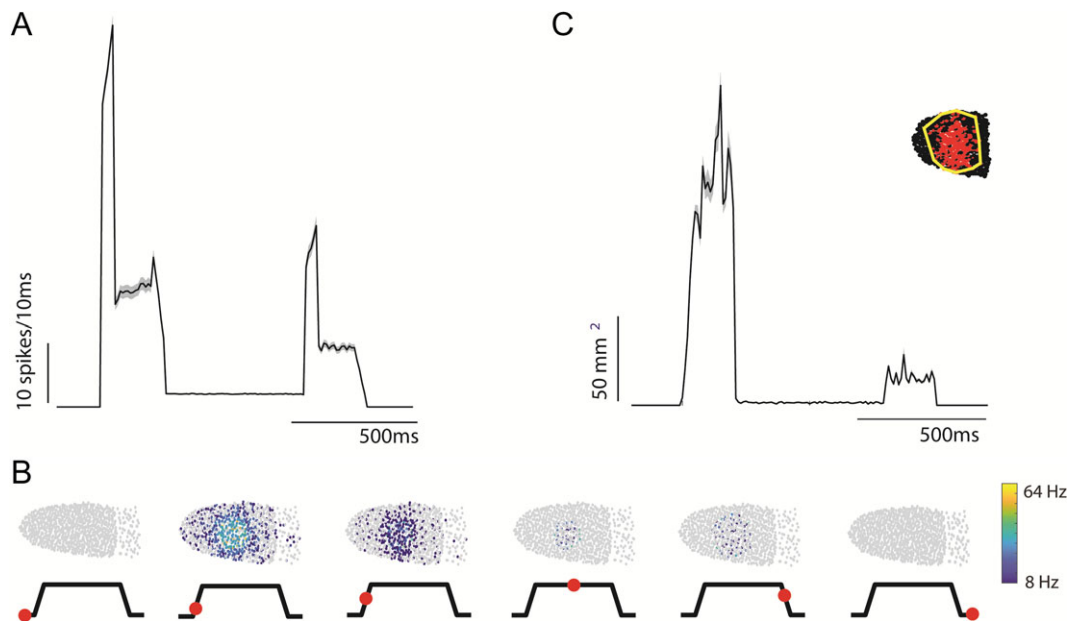


**Figure 8.** Spatiotemporal dynamics of peripheral responses to skin indentations. (A) Simulated aggregate afferent responses (SA1, RA, and PC fibers) to a 2-mm, 10-mm/s indentation delivered to various locations on the hand, matched to those used in the cortical experiments (see Supplementary Fig. S2). Spike count represents summed spikes over the afferent population, in 10-ms bins, averaged across locations (Supplementary Fig. S2: mean = 2498 fibers, stdev = 1369 fibers). Shaded area represents standard error of the mean over all locations ( $n = 16$ ). (B) Spatial pattern of the (stimulated) afferent activation during each epoch (indicated on the trace below). Each dot represents a receptive field of a tactile nerve fiber (SA1 and RA fibers only) on the distal index finger pad and the color of the dot denotes the fiber’s firing rate during the corresponding epoch. (C) Dynamics of the spatial extent of simulated afferent activation for 20-ms bins. Area was set to 0 for time points where less than 3 afferents were recruited, inset shows an example diagram of the polygon-based area computation.

peripheral and cortical PSTHs to the same stimuli and found these to be high (mean  $\pm$  s.d.:  $0.92 \pm 0.03$ ) (Supplementary Fig. S10). In conclusion, then, the spatiotemporal dynamics of cortical responses to simulated contact events are highly similar to their peripheral counterparts.

## Discussion

In summary, then, we found that population responses during the initiation and termination of contact dwarf responses during static contact both in the nerve and in cortex, so these responses signal primarily contact transients—changes in skin deformation—rather than tracking indentation depth. Furthermore, contact events are encoded in both the time-varying response of activated neurons as well as the time-varying size of the activated population. While responses to contact transients are strong and diffuse, responses to sustained contact are weak and highly localized. Information about the features of contact—its timing, location, and strength—are rapidly and faithfully conveyed by these phasic responses and can account for the ability of animals to discriminate indentations of varying strength. The spatiotemporal profile of the population response to contact in cortex mirrors its counterpart in the nerve.

### Encoding of Contact Location

As indentation rate or depth increases, the volume of activated neurons in somatosensory cortex increases, a phenomenon that has also been observed for increases in vibratory amplitude using optical intrinsic signal imaging (Simons et al. 2005). The recruitment of neurons during contact transients may seem to render localization more difficult if stimulus location is encoded in the spatial location of neuronal activity within the somatosensory homunculus. For example, 2 spatially restricted and minimally overlapping activation patterns would in principle be more distinguishable from one another than more diffuse, highly overlapping ones. Consistent with this, reducing the activated area through vibrotactile adaptation results in better localization performance (Tanan et al. 2006). However, we show that the centroid of neural activity remains consistent as the spatial extent of activation increases, so the hotzone remains consistent and dependent on contact location regardless of the other stimulation parameters (indentation depth and indentation rate). The stability of the hotzone provides a neural basis for the documented robustness of localization performance across changes in applied pressure (Gibson and Craig 2006) despite the concomitant changes in activated area. Thus, while increased activated area is intrinsically deleterious to localization, this effect is mitigated by the consistency of the hotzone location.

### Encoding of Indentation Rate

Increases in the rate at which the skin is indented results both in a systematic increase in firing rate of cortical neurons at the hotzone and in the recruitment of nearby neurons. The effect of indentation rate on the hotzone firing rate can be attributed primarily to RA and PC fibers whose responses are restricted to dynamic stimulus phases and increase as indentation rate increases, but SA1 afferents also respond more strongly to faster indentations (Knibestöl 1975; Pubols and Pubols 1976). That increases in indentation rate also result in an increase in the number of activated nerve fibers has been previously documented (Johnson 1974; Cohen and Vierck 1993; Muniak et al. 2008) and can be attributed to the increased sensitivity of rapidly adapting fibers at higher

speeds (Knibestöl 1973). That indentation rate is a major determinant of cortical responses is consistent with results from psychophysical experiments with human observers showing that indentation rate drives to a large extent the perceived intensity of an indentation (Poulos et al. 1984).

### Similarity of Peripheral and Cortical Response Dynamics

The aggregate response of cortical neurons to contact events is very similar to that of their peripheral inputs. First, the coarse temporal profiles of the spiking response is nearly identical to its cortical counterpart, featuring a prominent phasic response during contact transients and a weak tonic response during maintained contact. As alluded to above, a major source of the strong transient response in the nerve is the population of rapidly adapting afferents, including RA and PC fibers, which respond exclusively during the transients, and the stronger response of SA1 fibers during the indentation phase. Second, the dynamics of recruitment observed in cortex also seem to mirror those at the periphery. Indeed, phasic recruitment of nerve fibers originating from afferents close to but not under the probe is observed during the transient periods and only a small population of SA1 fibers with RFs just under the probe is activated during sustained contact. Not only are the relative strengths of the transient and sustained responses similar in periphery and cortex, but their dependence on the locus of stimulation is also consistent (with weaker sustained responses from the palm). Finally, the dependence of the spatiotemporal dynamics of nerve responses on stimulus parameters—including indentation depth and indentation rate—largely mirrors its cortical counterpart (Supplementary Fig. S10).

That the aggregate response in cortex resembles that in the nerve does not imply that no information processing occurs between nerve and cortex. Indeed, individual cortical neurons have complex RFs with excitatory and inhibitory subfields (DiCarlo et al. 1998), often exhibit feature selectivity (to edge orientation (Bensmaia et al. 2008) or direction of motion (Pei et al. 2010)), and integrate their inputs nonlinearly (Chung et al. 2002; Katz et al. 2006; Thakur et al. 2006; Reed et al. 2010, 2011; Brouwer et al. 2015; Saal et al. 2015) to name a few properties that are largely absent in tactile nerve fibers. Interestingly, however, this processing is largely obscured when pooling responses to contact events across populations of neurons.

### Active Versus Passive Touch

One might argue that the neuronal activity when stimuli are passively presented to the skin may not be representative of that evoked during active manipulation of objects. However, several lines of evidence suggest otherwise.

First, while the temporal profile of the indentations, following a trapezoidal trajectory, is highly contrived and may not match that of natural contact event, afferent responses to a natural indentation profile, corresponding to grasping and releasing a coffee cup, exhibit very similar spatiotemporal dynamics (Supplementary Fig. S7B).

Second, tactile discrimination and pattern recognition are similar for active and passive touch (Lamotte and Whitehouse 1986; Vega-Bermudez et al. 1991), suggesting that the processing of cutaneous information is similar under these 2 conditions.

Third, studies explicitly comparing responses of somatosensory neurons to active and passive touch have found weak or no differences in firing rates, and any observed differences could be attributed to differences in the contact

events themselves or in the attentional state of the animal (Chapman and Ageranioti-Belanger 1991; Jiang et al. 1991; Ageranioti-Bélanger and Chapman 1992; Williams and Chapman 2002). Regarding the former confound, comparing the neuronal responses to active and passive touch is challenging because it is impossible to exactly match how the skin is deformed in the 2 conditions and the sense of touch is exquisitely sensitive to any differences in skin deformation (down to the level of single-digit microns). Indeed, as discussed above, even under passive conditions, skin deflections produced by an identical stimulus are highly variable given the slight movements of the (restrained) hand, a challenge we circumvent by imposing a preindentation.

Fourth, while single-unit cortical responses evoked during grasping (Wannier et al. 1986, 1991; Gardner et al. 1999; Salimi et al. 1999; Ro et al. 2000; Debowy et al. 2001) are difficult to compare to aggregate cortical responses presented here, somatosensory neurons with RFs on the glabrous skin have been found to exhibit properties qualitatively consistent with those described here, often characterized by strong phasic responses at initiation and termination of contact and weak responses during maintenance of contact. Another component of active touch that may influence tactile responses in somatosensory cortex is movement-gating, a phenomenon that has been documented for the balance sense, vision, and touch (Cullen et al. 2004). However, while cortical responses to touch on the proximal limb are suppressed during movement, the response dynamics seem to be preserved (Jiang et al. 1990, 1991). Moreover, the function of movement gating of touch on the proximal limb may be to reduce tactile signals produced by skin stretch during movement (Rincon-Gonzalez et al. 2011), which, in some cases, may be behaviorally irrelevant and distracting. In this view, it is unlikely that tactile responses on the glabrous skin would be suppressed during object manipulation as these signals are the ones critical to behavior.

In light of these considerations and previous findings, we expect that the cutaneous responses to object contact in somatosensory cortex are unlikely to be fundamentally altered under conditions of active touch and that passive stimulation reveals the main characteristics of the representation of contact events at this stage of processing along the somatosensory neuraxis.

### Functional Significance of the Phasic Response to Contact Transients

Object manipulation can be broken down into a sequence of action phases delimited by mechanical events associated with subgoals of the task. In reach and grasp, for example, contact with an object marks the end of the reach phase and signals the beginning of the grasp phase (Johansson and Flanagan 2009). Consistent with this view, disruption of somatosensory cortex with a pulse of transcranial magnetic stimulation (TMS) just before contact results in delayed initiation of the grasp (Lemon et al. 1995). Moreover, contact timing between object and fingers drives the online adaptation of grasp aperture during active grasping movements (Säfstrom and Edin 2008). The prominence of contact transients in cortex is consistent with a role for tactile feedback in signaling transitions between task goals rather than providing continuous feedback about object interactions (Johansson and Edin 1993; Johansson and Flanagan 2009). We would therefore expect that these phasic transients are key components of sensorimotor integration during object manipulation.

This is not to say that sustained responses are not useful and informative. Indeed, stimulus features—local object shape, for

example,—may be most prominently encoded in cortical responses during sustained contact (Bensmaia et al. 2008; Yau et al. 2013). However, this slower signal may be less important for online motor control and play a greater role in haptic perception (Yau et al. 2016).

### Implications for Neuroprosthetics

Characterization of the spatiotemporal dynamics of the response to contact events not only sheds light on the neural coding of tactile information and the role of touch in guiding object interactions but also has implications for the design of sensory feedback algorithms for use in upper limb neuroprostheses. Indeed, a basic design principle of such algorithms is to evoke patterns of neuronal activation through electrical stimulation that mimic natural patterns as much as possible (Bensmaia 2015; Delhayé et al. 2016). To the extent that electrically induced neuronal activation matches its natural counterpart, the resulting percepts will be naturalistic and intuitive, so little to no training will be required to learn to interpret them.

The standard sensory encoding algorithm converts the output of pressure (or force) sensors on the bionic hand into trains of electrical stimulation whose frequency or amplitude is modulated according to the sensory output. Within this framework, the rate of change of pressure does not influence the stimulation regime. Our results suggest that, to mimic natural responses to contact events, both in the periphery and in cortex, it is preferable to track changes in pressure while only weakly weighting the instantaneous pressure in the determination of stimulation parameters. Furthermore, the encoding algorithm should not only yield an increase in firing rate at the hotzone electrode—perhaps achieved through an increase in stimulation frequency—but also in the recruitment of nearby neurons—achievable by modulating the amplitude of stimulation or by stimulating through a variable number of adjacent electrodes. The resulting electrically induced patterns of neuronal activation will have the merit of signaling contact timing with much greater precision than do the slowly evolving pressure-tracking algorithms (for the same reasons that the natural phasic responses are more temporally precise). Furthermore, the spatiotemporal dynamics of the response are liable to be more effectively integrated into motor planning and execution in that they reproduce key features of a natural cortical response to contact. We anticipate that such biomimetic stimulation patterns will lead to improved dexterity for bionic hands.

Another important implication of the present results for neuroprosthetics is that, given the remarkable similarities in the spatiotemporal dynamics of the aggregate response in periphery and cortex, sensory encoding algorithms developed for cortical interfaces may be very similar to those developed for the peripheral nerve interfaces (Okorokova et al. 2018).

### Supplementary Material

Supplementary material is available at *Cerebral Cortex* online.

### Funding

NIH, National Institute of Neurological Disorders and Stroke (NINDS) grants [R01 NS095251 (S.J.B.) and F31 NS096952 (A.K.S.)].

### Notes

We would like to thank Robert Gaunt and Benoit Delhayé for comments on a previous version of this manuscript. *Conflict of Interest:* None declared.

## References

- Ageranioti-Bélanger SA, Chapman CE. 1992. Discharge properties of neurones in the hand area of primary somatosensory cortex in monkeys in relation to the performance of an active tactile discrimination task. II. Area 2 as compared to areas 3b and 1. *Exp Brain Res.* 91:207–228.
- Augurelle A-S, Smith AM, Lejeune T, Thonnard J-L. 2003. Importance of cutaneous feedback in maintaining a secure grip during manipulation of hand-held objects. *J Neurophysiol.* 89:665–671.
- Bensmaia SJ. 2015. Biological and bionic hands: natural neural coding and artificial perception. *Philos Trans R Soc B Biol Sci.* 370:20140209.
- Bensmaia SJ, Denchev PV, Dammann JF III, Craig JC, Hsiao SS. 2008. The representation of stimulus orientation in the early stages of somatosensory processing. *J Neurosci.* 28:776–786.
- Britten KH, Shadlen MN, Newsome WT, Movshon JA. 1992. The analysis of visual motion: a comparison of neuronal and psychophysical performance. *J Neurosci.* 12:4745–4765.
- Brochier T, Boudreau MJ, Paré M, Smith AM. 1999. The effects of muscimol inactivation of small regions of motor and somatosensory cortex on independent finger movements and force control in the precision grip. *Exp Brain Res.* 128:31–40.
- Brouwer GJ, Arnedo V, Offen S, Heeger DJ, Grant AC. 2015. Normalization in human somatosensory cortex. *J Neurophysiol.* 114:2588–2599.
- Callier T, Schluter EW, Tabot GA, Miller LE, Tenore FV, Bensmaia SJ. 2015. Long-term stability of sensitivity to intracortical microstimulation of somatosensory cortex. *J Neural Eng.* 12:056010.
- Carlson M. 1981. Characteristics of sensory deficits following lesions of Brodmann's areas 1 and 2 in the postcentral gyrus of Mocooco mulatto. *Brain Res.* 204:424–430.
- Chapman CE, Ageranioti-Belanger A. 1991. Experimental brain research discharge properties of neurones in the hand area of primary somatosensory cortex in monkeys in relation to the performance of an active tactile discrimination task I. Areas 3b and 1. *Exp Brain Res.* 87:31–339.
- Chung S, Li X, Nelson SB. 2002. Short-term depression at thalamocortical synapses contributes to rapid adaptation of cortical sensory responses in vivo. *Neuron.* 34:437–446.
- Cohen R, Vierck C. 1993. Population estimates for responses of cutaneous mechanoreceptors to a vertically indenting probe on the glabrous skin of monkeys. *Exp Brain Res.* 94:105–119.
- Cullen KE, Anderson ME, Kiehn O. 2004. Sensory signals during active versus passive movement. *Curr Opin Neurobiol.* 14:698–706.
- Debowy DJ, Ghosh S, Gardner EP, Ro JY. 2001. Comparison of neuronal firing rates in somatosensory and posterior parietal cortex during prehension. *Exp Brain Res.* 137:269–291.
- Delhaye BP, Saal HP, Bensmaia SJ. 2016. Key considerations in designing a somatosensory neuroprosthesis. *J Physiol.* 110:402–408.
- DiCarlo JJ, Johnson KO, Hsiao SS. 1998. Structure of receptive fields in area 3b of primary somatosensory cortex in the alert monkey. *J Neurosci.* 18:2626–2645.
- Dong Y, Mihalas S, Kim SS, Yoshioka T, Bensmaia S, Niebur E. 2013. A simple model of mechanotransduction in primate glabrous skin. *J Neurophysiol.* 109:1350–1359.
- Duque J, Thonnard J, Vandermeeren Y, Sèbire G, Cosnard G, Olivier E. 2003. Correlation between impaired dexterity and corticospinal tract dysgenesis in congenital hemiplegia. *Brain.* 126:732–747.
- Flesher SN, Collinger JL, Foldes ST, Weiss JM, Downey JE, Tyler-Kabara EC, Bensmaia SJ, Schwartz AB, Boninger ML, Gaunt RA. 2016. Intracortical microstimulation of human somatosensory cortex. *Sci Transl Med.* 8:361ra141.
- Gardner EP, Ro JY, Debowy D, Ghosh S. 1999. Facilitation of neuronal activity in somatosensory and posterior parietal cortex during prehension. *Exp Brain Res.* 127:329–354.
- Gibson GO, Craig JC. 2006. The effect of force and conformance on tactile intensive and spatial sensitivity. *Exp Brain Res.* 170:172–181.
- Goodman JM, Bensmaia SJ. 2017. A variation code accounts for the perceived roughness of coarsely textured surfaces. *Sci Rep.* 7:46699.
- Hikosaka O, Tanaka M, Sakamoto M, Iwamura Y. 1985. Deficits in manipulative behaviors induced by local injections of muscimol in the first somatosensory cortex of the conscious monkey. *Brain Res.* 325:375–380.
- Hyvarinen J, Poranen A, Jokinen Y. 1980. Influence of attentive behavior on neuronal responses to vibration in primary somatosensory cortex of the monkey. 43.
- Iwamura Y, Tanaka M, Sakamoto M, Hikosaka O. 1983. Converging patterns of finger representation and complex response properties of neurons in area 1 of the first somatosensory cortex of the conscious monkey. *Exp Brain Res.* 51:327–337.
- Jiang W, Chapman CE, Lamarre Y. 1990. Modulation of somatosensory evoked responses in the primary somatosensory cortex produced by intracortical microstimulation of the motor cortex in the monkey. *Exp Brain Res.* 80:333–344.
- Jiang W, Chapman CE, Lamarre Y. 1991. Modulation of the cutaneous responsiveness of neurones in the primary somatosensory cortex during conditioned arm movements in the monkey. *Exp Brain Res.* 84:342–354.
- Johansson RS, Edin BB. 1993. Predictive feed-forward sensory control during grasping and manipulation in man. *Biomed Res.* 14:95–106.
- Johansson RS, Flanagan JR. 2009. Coding and use of tactile signals from the fingertips in object manipulation tasks. *Nat Rev Neurosci.* 10:345–359.
- Johansson RS, Vallbo AB. 1979. Tactile sensibility in the human hand: relative and absolute densities of four types of mechanoreceptive units in glabrous skin. *J Physiol.* 286:283–300.
- Johnson KO. 1974. Reconstruction of population response to a vibratory stimulus in quickly adapting mechanoreceptive afferent fiber population innervating glabrous skin of the monkey. *J Neurophysiol.* 37:48–72.
- Johnson KO, Phillips JR. 1981. Tactile spatial resolution. I. Two-point discrimination, gap detection, grating resolution, and letter recognition. *J Neurophysiol.* 46:1177–1192.
- Kaas JH. 1983. What, if anything, is SI? Organization of first somatosensory area of cortex. *Physiol Rev.* 63:206–231.
- Katz Y, Heiss JE, Lampl I. 2006. Cross-whisker adaptation of neurons in the rat barrel cortex. *J Neurosci.* 26:13363–13372.
- Kim SS, Mihalas S, Russell A, Dong Y, Bensmaia SJ. 2011. Does afferent heterogeneity matter in conveying tactile feedback through peripheral nerve stimulation? *IEEE Trans Neural Syst Rehabil Eng.* 19:514–520.
- Knibestöl M. 1973. Stimulus-response functions of rapidly adapting mechanoreceptors in the human glabrous skin area. *J Physiol.* 232:427–452.
- Knibestöl M. 1975. Stimulus-response functions of slowly adapting mechanoreceptors in the human glabrous skin area. *J Physiol.* 245:63–80.

- Lamotte RH, Whitehouse J. 1986. Tactile detection of a dot on a smooth surface: peripheral neural events. *J Neurophysiol.* 56:1109–1128. Printed in USA.
- Lemon RN, Johansson RS, Westling G. 1995. Corticospinal control during reach, grasp, and precision lift in man. *J Neurosci.* 15:6145–6156.
- Mathis MW, Mathis A, Uchida N. 2017. Somatosensory cortex plays an essential role in forelimb motor adaptation in mice. *Neuron.* 93:1493–1503.e6.
- Muniak MA, Ray S, Hsiao SS, Dammann JF, Bensmaia SJ. 2008. The neural coding of stimulus of mechanoreceptive afferents with psychophysical behavior. *J Neurosci.* 27:11687–11699.
- Meftah E-M, Shenasa J, Chapman CE. 2002. Effects of a cross-modal manipulation of attention on somatosensory cortical neuronal responses to tactile stimuli in the monkey. *J Neurophysiol.* 88:3133–3149.
- Okorokova L, He Q, Bensmaia SJ. 2018. Biomimetic encoding model for restoring touch in bionic hands through a nerve interface. *J Neural Eng.* 15:066033.
- Ostry DJ, Darainy M, Mattar AAG, Wong J, Gribble PL. 2010. Somatosensory plasticity and motor learning. *J Neurosci.* 30:5384–5393.
- Pei Y-C, Hsiao SS, Craig JC, Bensmaia SJ. 2010. Shape invariant coding of motion direction in somatosensory cortex. *PLoS Biol.* 8:e1000305.
- Penfield W, Brain E. 1937. Somatic motor and sensory representation in the cerebral cortex of man as studied by electrical stimulation. *Brain.* 60:389–443.
- Pons TP, Garraghty PE, Cusick CG, Kaas JH. 1985. A sequential representation of the occiput, arm, forearm and hand across the rostrocaudal dimension of areas 1, 2 and 5 in macaque monkeys. *Brain Res.* 335:350–353.
- Poulos DA, Mei J, Horch KW, Tuckett RP, Wei JY, Cornwall MC, Burgess PR, Evans B, Fisher J, Frederickson G, et al. 1984. The neural signal for the intensity of a tactile stimulus. *J Neurosci.* 4:2016–2024.
- Pubols BH, Pubols LM. 1976. Coding of mechanical stimulus velocity and indentation depth by squirrel monkey and raccoon glabrous skin mechanoreceptors. *J Neurophysiol.* 39:773–787.
- Rajan AT, Boback JL, Dammann JF, Tenore FV, Wester BA, Otto KJ, Gaunt RA, Bensmaia SJ. 2015. The effects of chronic intracortical microstimulation on neural tissue and fine motor behavior. *J Neural Eng.* 12:066018.
- Reed JL, Pouget P, Qi H-X, Zhou Z, Bernard MR, Burish MJ, Haitas J, Bonds AB, Kaas JH. 2008. Widespread spatial integration in primary somatosensory cortex. *Proc Natl Acad Sci USA.* 105:10233–10237.
- Reed JL, Qi H-X, Kaas JH. 2011. Spatiotemporal properties of neuron response suppression in owl monkey primary somatosensory cortex when stimuli are presented to both hands. *J Neurosci.* 31:3589–3601.
- Reed JL, Qi H-X, Zhou Z, Bernard MR, Burish MJ, Bonds AB, Kaas JH. 2010. Response properties of neurons in primary somatosensory cortex of owl monkeys reflect widespread spatio-temporal integration. *J Neurophysiol.* 103:2139–2157.
- Rincon-Gonzalez L, Warren JP, Meller DM, Helms Tillery S. 2011. Haptic interaction of touch and proprioception: implications for neuroprosthetics. *IEEE Trans Neural Syst Rehabil Eng.* 19:490–500.
- Ro JY, Debowy D, Ghosh S, Gardner EP. 2000. Depression of neuronal firing rates in somatosensory and posterior parietal cortex during object acquisition in a prehension task. *Exp Brain Res.* 135:1–11.
- Saal HP, Delhaye BP, Rayhaun BC, Bensmaia SJ. 2017. Simulating tactile signals from the whole hand with millisecond precision. *Proc Natl Acad Sci USA.* 114:E5693–E5702.
- Saal HP, Harvey MA, Bensmaia SJ. 2015. Rate and timing of cortical responses driven by separate sensory channels. *Elife.* 4:e10450.
- Salimi I, Brochier T, Smith AM. 1999. Neuronal activity in somatosensory cortex of monkeys using a precision grip. I. Receptive fields and discharge patterns. *J Neurophysiol.* 81:825–834.
- Schabrun SM, Ridding MC, Miles TS. 2008. Role of the primary motor and sensory cortex in precision grasping: a transcranial magnetic stimulation study. *Eur J Neurosci.* 27:750–756.
- Simons SB, Tannan V, Chiu J, Favorov OV, Whitsel BL, Tommerdahl M. 2005. Amplitude-dependency of response of SI cortex to flutter stimulation. *BMC Neurosci.* 6:43.
- Sripati AP, Yoshioka T, Denchev P, Hsiao SS, Johnson KO. 2006. Spatiotemporal receptive fields of peripheral afferents and cortical area 3b and 1 neurons in the primate somatosensory system. *J Neurosci.* 26:2101–2114.
- Sur M, Wall JT, Kaas JH. 1981. Modular segregation of functional cell classes within the postcentral somatosensory cortex of monkeys. *Science.* 212:1059–1061.
- Säfström D, Edin BB. 2008. Prediction of object contact during grasping. *Exp Brain Res.* 190:265–277.
- Tabot GA, Dammann JF, Berg JA, Tenore FV, Boback JL, Vogelstein RJ, Bensmaia SJ. 2013. Restoring the sense of touch with a prosthetic hand through a brain interface. *Proc Natl Acad Sci USA.* 110:18279–18284.
- Tanan V, Whitsel BL, Tommerdahl M. 2006. Vibrotactile adaptation enhances spatial localization. *Brain Res.* 1102:109–116.
- Thakur PH, Fitzgerald PJ, Lane JW, Hsiao SS. 2006. Receptive field properties of the macaque second somatosensory cortex: nonlinear mechanisms underlying the representation of orientation within a finger pad. *J Neurosci.* 26:13567–13575.
- Vega-Bermudez F, Johnson KO. 1999. Surround suppression in the responses of primate SA1 and RA mechanoreceptive afferents mapped with a probe array. *J Neurophysiol.* 81:2711–2719.
- Vega-Bermudez F, Johnson KO, Hsiao SS. 1991. Human tactile pattern recognition: active versus passive touch, velocity effects, and patterns of confusion. *J Neurophysiol.* 65:531–546.
- Wannier TM, Maier MA, Hepp-Reymond MC. 1991. Contrasting properties of monkey somatosensory and motor cortex neurons activated during the control of force in precision grip. *J Neurophysiol.* 65:572–589.
- Wannier TMJ, Törtl M, Hepp-Reymond M-C. 1986. Neuronal activity in the postcentral cortex related to force regulation during a precision grip task. *Brain Res.* 382:427–432.
- Williams SR, Chapman CE. 2002. Time course and magnitude of movement-related gating of tactile detection in humans. III. Effect of motor tasks. *J Neurophysiol.* 88:1968–1979.
- Witney AG, Wing A, Thonnard J-L, Smith AM. 2004. The cutaneous contribution to adaptive precision grip. *Trends Neurosci.* 27:637–643.
- Xerri C, Merzenich MM, Peterson BE, Jenkins W. 1998. Plasticity of primary somatosensory cortex paralleling sensorimotor skill recovery from stroke in adult monkeys. *J Neurophysiol.* 79:2119–2148.
- Yau JM, Connor CE, Hsiao SS. 2013. Representation of tactile curvature in macaque somatosensory area 2. *J Neurophysiol.* 109:2999–3012.
- Yau JM, Kim SS, Thakur PH, Bensmaia SJ. 2016. Feeling form: the neural basis of haptic shape perception. *J Neurophysiol.* 115:631–642.